Supporting Material

Magnesium-antimony liquid metal battery for stationary energy storage

David J. Bradwell, Hojong Kim, Aislinn H. C. Sirk, Donald R. Sadoway

Experimental

Materials and methods:

The Mg||Sb cells comprised a graphite crucible, insulating sheath, current collector, current leads, and a cell cap (Figure S1). The graphite crucible was constructed from a 38 mm diameter and 90 mm long graphite rod (fine extruded grade, GraphiteStore.com, Inc.) into which was drilled a 19 mm diameter hole, 57 mm deep. A 19 mm diameter hot pressed boron nitride (BN) rod (Saint Gobain Advanced Ceramics) was machined into a tube with an inner diameter of 16 mm. Due to the poor wetting of Sb on graphite, a 3 mm diameter, 15 mm tungsten (Alfa Aesar) rod was compression fit into a 3 mm diameter hole in the bottom of the graphite crucible to serve as the positive current collector. A 6 mm diameter, 30 mm long SS rod (type 309 SS, McMaster Carr Supply Company) served as the negative current collector and was secured to a 3 mm diameter, 600 mm long SS rod (type 18-8 SS threaded rod, McMaster Carr Supply Company) which served as the negative electrode lead. A threaded hole was machined into the top lip of the graphite crucible, into which was secured a 600 mm long, 3 mm diameter SS rod (type 18-8 SS threaded rod, McMaster Carr Supply Company). This rod served as the positive electrode current lead.

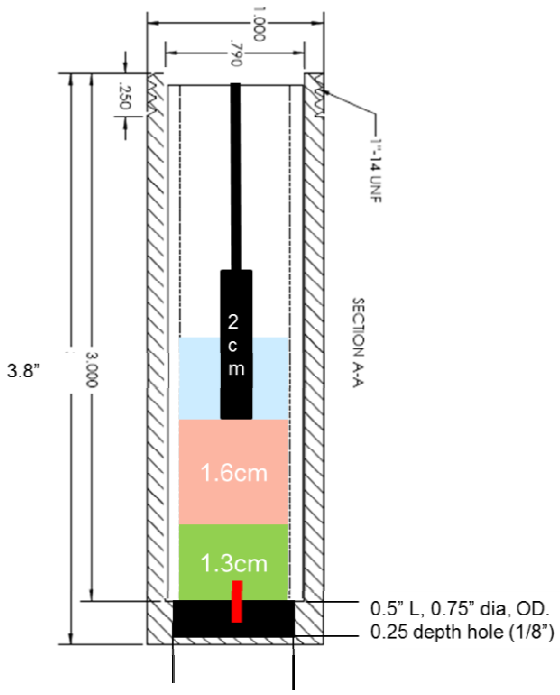

Figure S1. Scaled schematic of a Mg||Sb cell. units in inches, unless otherwise noted.

Assembly of the Mg||Sb cell was performed in an argon filled glove box. The W rod, graphite plug, and BN sheath were inserted into the graphite crucible. Sb granules (Alfa-Aesar, 99.5 % purity) were placed in the bottom of the crucible, the electrolyte salts were added, and Mg slugs (Alfa Aesar, 99.95 % purity) were placed on top of the salt. The dimensions and amount of materials used in two of the tested cells are included below (Table S1).

Table S1: Cell Dimensions, Materials and Operating Capacity.

	Cell A	**Cell B**	**Cell C**
Cell inner diameter (cm)	**1.63**	**1.63**	**1.63**
Area (cm^2)	**2.01**	**2.01**	**2.01**
Salt ($MgCl_2$-KCl-NaCl) weight (gram)	***5.79***	***6.91***	***9.98***
Salt height ($MgCl_2$-KCl-NaCl) (mm)	**13.61**	**15.88**	**30**
Sb weight (gram)	***17.00638 (+0.36687g Mg)***	***17.00187 (+0.36101g Mg)***	***17.0074 (+0.35004g Mg)***
Sb (mol)	**0.14**	**0.14**	**0.14**
Sb height (cm)	**1.30**	**1.30**	**1.30**
Mg weight (gram)	***2.98***	***2.99***	***1.47***
Mg (mol)	**0.12**	**0.12**	**0.06**
Mg height (cm)	**0.94**	**0.95**	**0.46**
Mg in Sb(mol%)	**49**	**49**	**35**
Maximum capacity (Ah)	**7.0**	**7.0**	**4.0**

Assembled cells were placed inside a 600 mm tall and 10 cm diameter stainless steel test vessel which was sealed using compression o-ring fittings. Current leads from the cell extended up through vacuum fittings in the cap of the test vessel, allowing electrochemical equipment to connect to the battery. A thermocouple was included to measure the temperature of the Mg||Sb cell. The sealed test vessel was removed from the glovebox and placed inside of a vertical tube furnace and the top of the test vessel was water cooled. The vessel was heated to 80 °C under vacuum and held for 12 h, then heated to 240 °C and held for an additional 12 h to dry. The vessel was backfilled with argon and heated to 700 °C at a rate of 5 °C/min, above the melting point of the Mg and Sb metal electrodes and salt electrolyte (Figure S2).

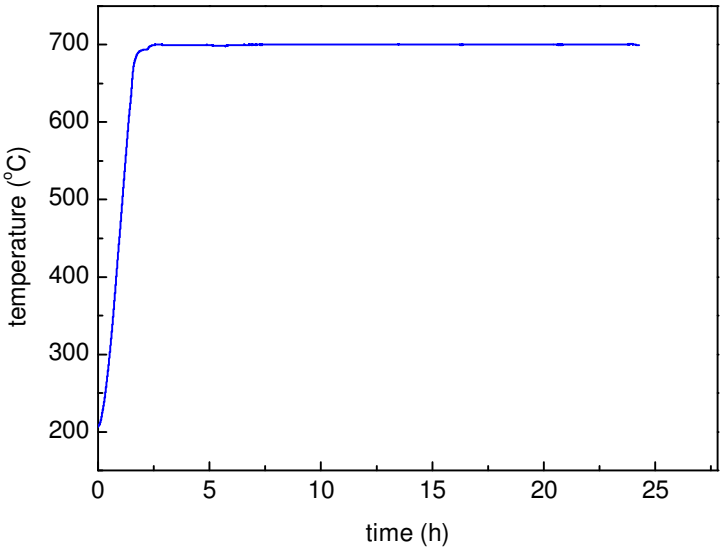

Figure S2. Heating profile of assembled cells in the test chamber.

Equipment:

Cyclic voltammetry, electrochemical impedance spectroscopy, and galvanostatic (constant current) battery cycling were performed using a Autolab potentiostat galvanostat model PGSTAT302N controlled by Nova v1.6 software. Leakage current measurements and battery cycling was performed using a Maccor 4300 Battery Tester with Mactest 32 control software and MIMS client v1.4 as the data collection and information management software. SEM/EDS analysis was performed using a Leo 438VP scanning electron microscope operated at 20 kV, with the EDS system was controlled by EDS2004 software.

Materials Choices

Materials Properties: Metals and Electrolyte

The metals and electrolyte were chosen based on a compatible range of material properties (density, melting point, immiscibility of metal, solubility of Mg^{2+} ions). These choices then informed the choice of containment materials.

The density of liquid Mg (1.6 g/ml)[1] is slightly less dense than these liquid salts, which have extrapolated liquid densities of 1.8 g/ml for NaCl, 1.6 g/ml for KCl at 600 °C.[2] The bottom layer comprised of liquid Sb has a density of 6.45 g/mL.[3] To facilitate Mg^{2+} transport through the electrolyte, $MgCl_2$ was included. The melting points of 650 °C, 630 °C, and 396 °C for Mg, Sb, and the electrolyte, respectively, are all well below the operating temperature of 700 °C thus ensuring a fully molten system. The voltage difference between the Sb and Mg is 0.44 V. The estimated voltages of other metals couples are included below (Table S2).

Table S2: Voltage of various metal couples. Voltage values were measured against the pure alkali or alkaline earth metal. Potentials were measured at different temperatures, and at different compositions (ranging from 10 mol% to 30 mol%), depending on the literature source. Systems of interest that have not yet been investigated, are indicated by NA (not available).

Voltage (V)	Bi	Te	Sb
Li	0.7[4]	1.7[5]	0.9[4]
Na	0.6 [5]	1.65 [6]	0.9[7]
Mg	0.34[8]	NA	0.47[8]

Mild steel was found to be a suitable current collector for the Mg electrode, as demonstrated by its use as a cathode in industrial Mg electrolysis cells.[9] Mg is capable of reducing Si from quartz (SiO_2), but alumina (Al_2O_3) and magnesia (MgO) are stable with liquid Mg and are suitable as insulating materials. Boron nitride (BN) is also stable and is easy to machine, so it was used as the insulating sheath.

Liquid Sb is more challenging to contain than liquid Mg because it dissolves structural metals, such as Fe and Ni.[10] W could be used as a current collector, but it is expensive and

difficult to machine. Fortunately, graphite was found to be stable with Mg, Sb, and molten halide salts and was therefore chosen as the crucible / lower electrode material.

Materials Cost and Abundance: Metals

The use of Sb as the positive liquid electrode in an liquid metal battery offers a low-cost chemistry, below the threshold cost required for broad-scale adoption of a large-scale electricity storage technology.[11] Antimony could potentially drop the cost of the active components by a factor of five (Table S3), while providing similar voltages for analogous chemistries (Table S2). Molten chlorifde salts, such as $MgCl_2$, KCl, and NaCl are suitable as the electrolyte, providing high conductivity, a suitable density and liquid range, and stability with reactive metals.

Table S3: Candidate electrode material cost and world reserves. Information collected from USGS Mineral Commodity Summaries[12], unless otherwise noted.

Metal	Electrode	Cost ($/kg)	Cost ($/mol)	World reserves (10^3 tons)
Li	negative	65[13]	0.4	9,900
Na	negative	1.6[14]	0.04	>1,000,000
Mg	negative	5	0.13	>1,000,000
Bi	positive	24	4.4	330
Te	positive	150	19	21
Sb	positive	7	0.74	2,100

Electrochemistry

Open Circuit Voltage

The open circuit voltage was measured as the cells were heated. Cells were assembled in a partially charged state with ca. 0.36 g Mg added to ca. 17 g Sb. The open circuit voltage was stable and reproducible at 0.44 V (Figure S3), as expected from calculated thermodynamic values.[15]

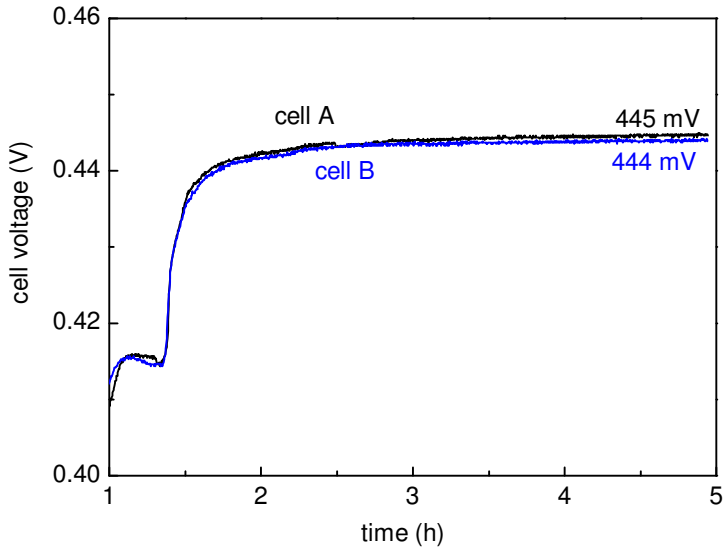

Figure S3: Open circuit voltage of Mg||Sb liquid metal battery (Cell A and Cell B) while heated to 700°C, prior to being charged and discharged.

Internal Resistance

The electrical resistance of the electrolyte was found to be the dominant form of overpotential based on cyclic voltammetry and electrochemical impedance spectroscopy. A cyclic voltammogram (Figure S4a) demonstrated a linear response, indicating facile charge transfer kinetics and minimal mass transport kinetics. Electrochemical impedance spectroscopy (Figure S4b) indicated negligible charge transfer resistance. Both graphs indicate that the ohmic resistance was in the range of 1.1 Ω cm^2, which is low, but is the only significant contribution to overpotential (ohmic).

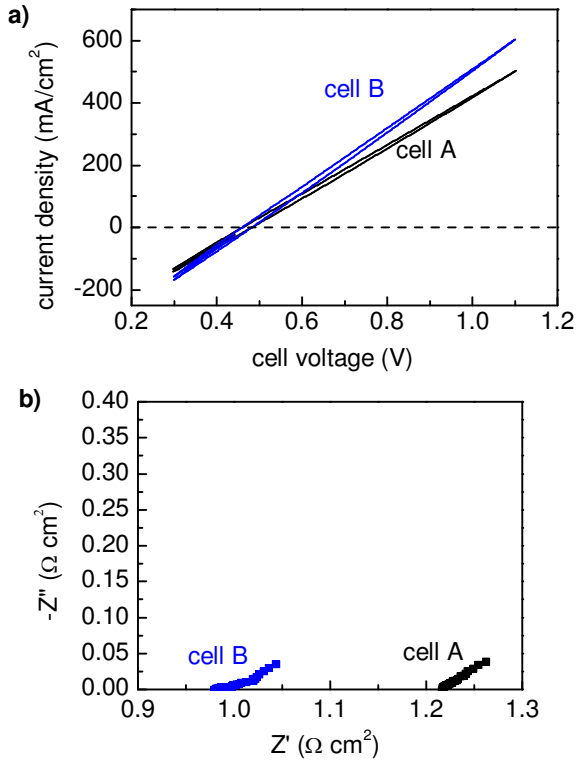

Figure S4: Electrochemical analysis of an Mg||Sb cell. a) Cyclic voltammogram. Scan rate 20 mV/s. b) Electrochemical impedance spectroscopy of cell in intermediate charge state. Scan parameters: voltage amplitude of 0.1 V rms; frequency range, 139 Hz to 0.1 Hz (cell A), 72 Hz to 0.1 Hz (cell B).

Leakage Current

The leakage current measured by stepped-potential measurements was < 1 mA/cm^2 (Figure S5).

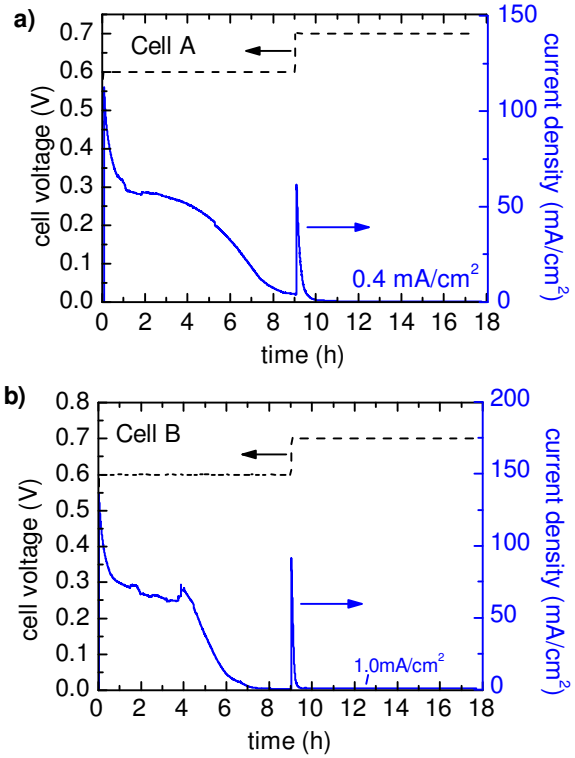

Figure S5: Stepped potential measurements of Mg||Sb liquid metal battery at 700°C demonstrating leakage currents of 0.4 mA/cm^2 to 1.0 mA/cm^2 while being held at 0.7 V (above the fully charged OCV). Cell A and Cell B both had active positive electrode surface areas of 2 cm^2.

In other similarly constructed cells, the leakage current was calculated based on the relative amounts of charge passed during consecutive charge and discharge and was also estimated to be 1 mA/cm^2 (Figure S6).

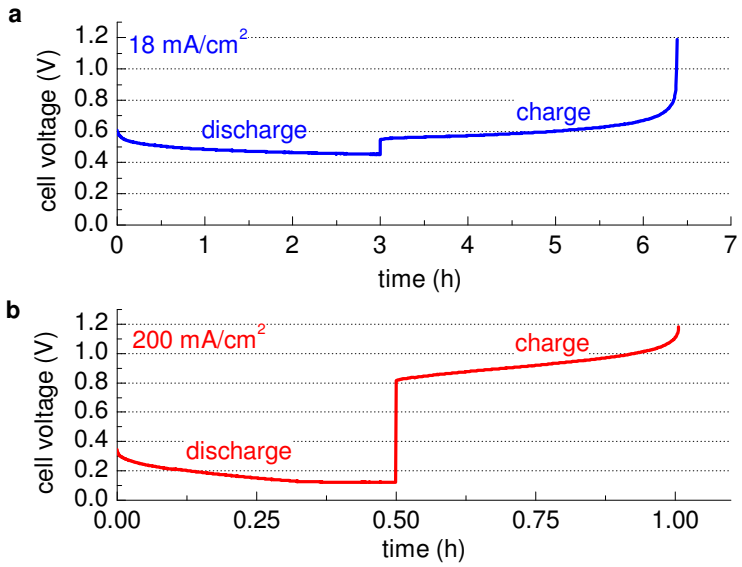

Figure S6: Mg||Sb cell cycle data. A) Cell cycled at $i = 18$ mA/cm^2. b) Cell cycled at $i = 200$ mA/cm^2. Cell was operated at 700 °C. Cell was assembled with 20 g of Sb, and 2 g of Mg, and 13.8 g of electrolyte (50:20:30 mol% $MgCl_2$:KCl:NaCl, resulting in an electrolyte thickness of ~1 cm), with an electroactive cross sectional area of 2.8 cm^2.

This low level of leakage current measured by two methods is impressive, and sufficiently low for grid-scale applications. As subsequent work on similarly constructed Na-based top electrode exhibited a significantly larger leakage current density (~50 mA/cm^2), this suggests that the complexing of Mg^{2+} by NaCl and KCl ligand donors effectively suppressed Mg metal solubility in the electrolyte as predicted from literature.[15]

Chronoamperometry.

For most experiments, constant current charge and discharge was used to simulate actual battery charge and discharge. In contrast, the steady-state current at constant voltages had somewhat poor cell-to-cell consistency and were very sensitive to small changes in the negative electrode design in Mg-Sb cell, likely due to the wetting properties of liquid Mg on the current collector.

As expected, charging a cell at constant voltage of 0.65V results in a lower steady state current (4.3 mA/cm^2) than charging at 0.75 V (4.7 mA/cm^2).

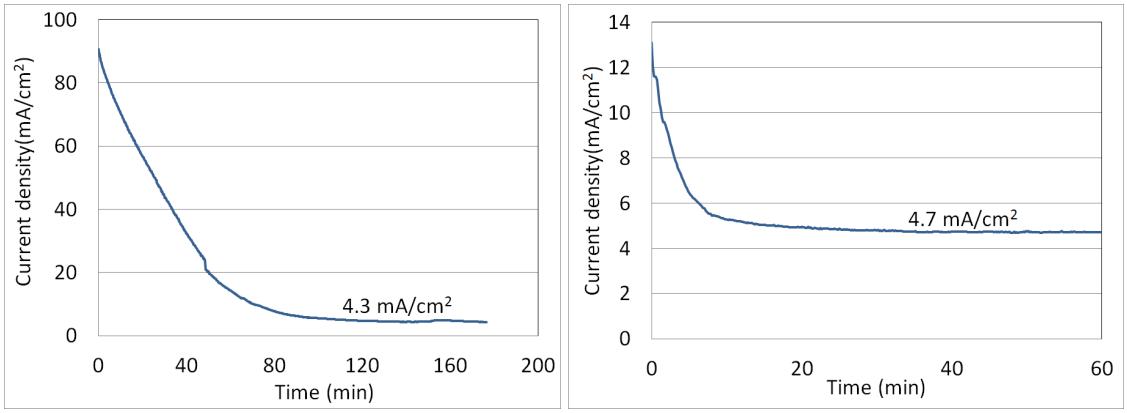

Figure S7: Mg||Sb cell cycle data. Electrochemical analysis of an Mg||Sb cell. a) Chronoamperometric charge of Cell C at 0.65 V resulting in a steady state current of 4.3 A/cm2. b) Chronoamperometric charge of Cell C at 0.75 V resulting in a steady state current of 4.7 A/cm2.

References:

[1] McGonigal, P., A. Kirshenbaum, and A. Grosse, The liquid temperature range, density, and critical constants of magnesium. The Journal of Physical Chemistry, 1962. 66(4): p. 737-740.

[2] Janz, G., Molten salt handbook. 1967, Academic Press, New York.

[3] Lianwen Wang *et al* Precise measurement of the densities of liquid Bi, Sn, Pb and Sb *J. Phys* 2003*.: Condens. Matter* **15** 777

[4] Weppner, W. and R.A. Huggins, *Thermodynamicproperties of the intermetallic systems lithium-antimony and lithium-bismuth.* Journal of The Electrochemical Society, 1978. **125**(1): p. 7.

[5] Cairns, E.J., et al., *Galvanic cells with fused-salt electrolytes*. 1967, Argonne National Laboratory.

[6] Morachesvkii, A.G., E.A. Maiorova, N.M. Romanchenko, and M.V. Kozlova, *Thermodynamic properties of the sodium-tellurium system.* J. Appl. Chem. USSR, 1982. **55**(3): p. 481-484.

[7] Lantratov, M.F., Skirstymonskaya, B. I., *Depolarisation during deposition of alkali metals on liquid cathodes.* Russian Journal of Physical Chemistry, 1962. **36**(11): p. 1323-1326.

[8] Eckert, C., R. Irwin, and J. Smith, *Thermodynamic activity of magnesium in several highly-solvating liquid alloys.* Metallurgical and Materials Transactions B, 1983. **14**(3): p. 451-458.

[9] Jarrett, N., Advances in the smelting of magnesium. Alcoa Laboratories, 1981: p. 159-168.

[10] Alloy phase diagram center, ASM international. [cited June, 2010] Access date; Available from: http://www.asminternational.org/asmenterprise/apd/.

[11] Bradwell, D., Sadoway, D. & Ceder, G. *Technical and economic feasibility of a high-temperature self-assembling battery* Master of Engineering thesis, Massachusetts Institute of Technology, (2006).

[12] *U.S. geological survey (USGS), mineral commodity summaries*, in *U.S. Government Printing Office, Reston, Virginia, United States*. 2010, Minerals Information Team

[13] *MetalPrices.com*. 2010.

[14] *Inner Mongolia Lantai Industrial Co., Ltd* [June 25, 2010]; Available from: http://www.lantaicn.com/.

[15] Eckert, C.; Irwin, R. ; Smith, *J. Metall. Mater. Trans. B* **1983**, *14*, 451.